Supplementary Material

Amorphous Surface Layer *versus* Transient Amorphous Precursor Phase in Bone - A Case Study Investigated by Solid-state NMR Spectroscopy

Stanislas Von Euw,[a] Widad Ajili,[a] Tsou-Hsi-Camille Chan-Chang,[a] Annette Delices,[a] Guillaume Laurent,[a] Florence Babonneau,[a] Nadine Nassif[a] and Thierry Azaïs[a*]

[a] *Sorbonne Universités, UPMC Univ Paris 06, CNRS, Collège de France, Laboratoire de Chimie de la Matière Condensée de Paris (LCMCP), 4 place Jussieu, F-75005, Paris, France.*

*corresponding author: thierry.azais@upmc.fr; +33 1 44 27 56 75

This PDF file includes Figures S1 to S11and Table S1.

Figure S1

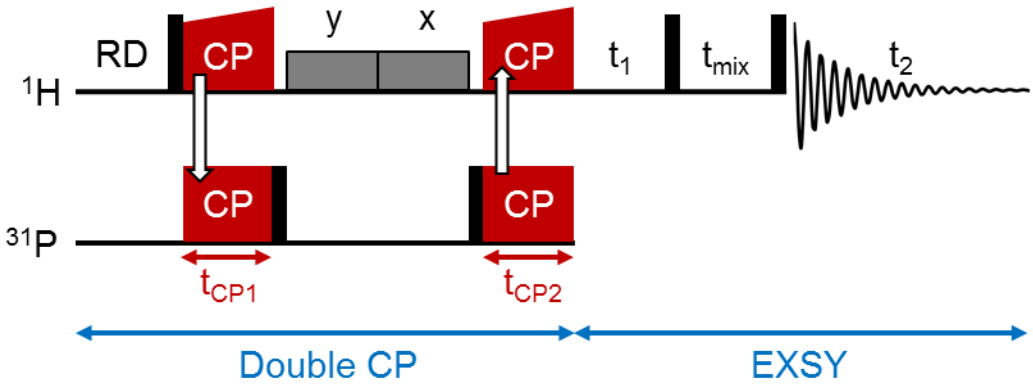

Figure S1. Schematic pulse sequence of the ^{1}H Double CP EXSY MAS NMR experiment that consists of a Double CP ^{1}H→^{31}P→^{1}H experiment followed by a ^{1}H magnetization EXchange SpectroscopY (EXSY) experiment.

Figure S2

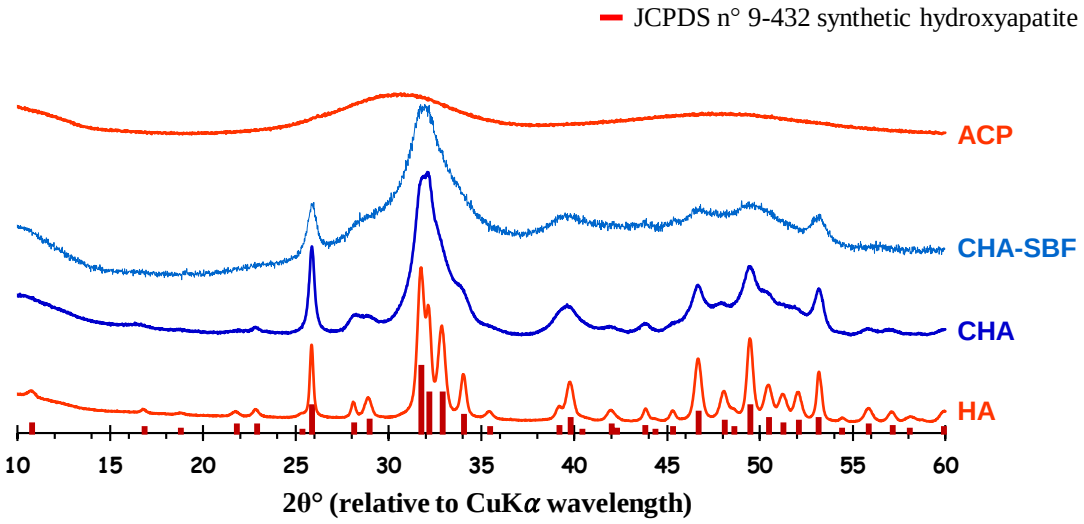

Figure S2. Powder XRD patterns of the synthetic calcium phosphate samples: stoichiometric apatite (**HA**); biomimetic apatites (**CHA** and **CHA-SBF**); and amorphous calcium phosphate (**ACP**).

Figure S3

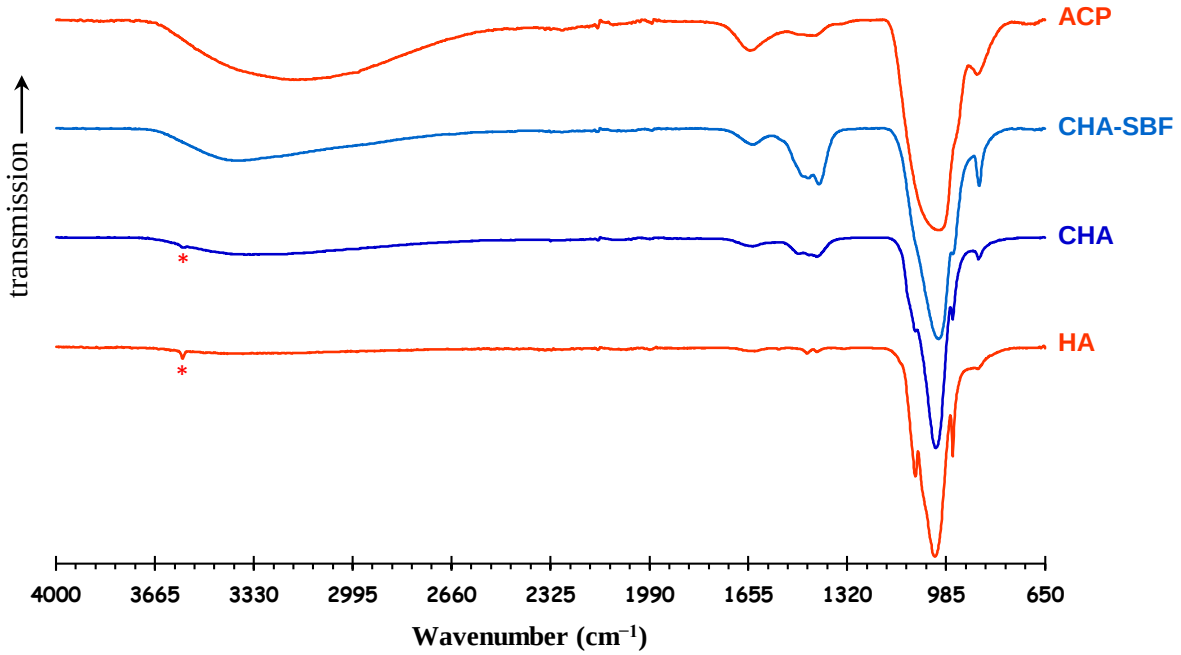

Figure S3. FT-IR spectra of the synthetic calcium phosphate samples: stoichiometric apatite (**HA**); biomimetic apatites (**CHA** and **CHA-SBF**); and amorphous calcium phosphate (**ACP**). Red asterisks = hydroxyl ions located in crystalline apatitic environments.

Figure S4

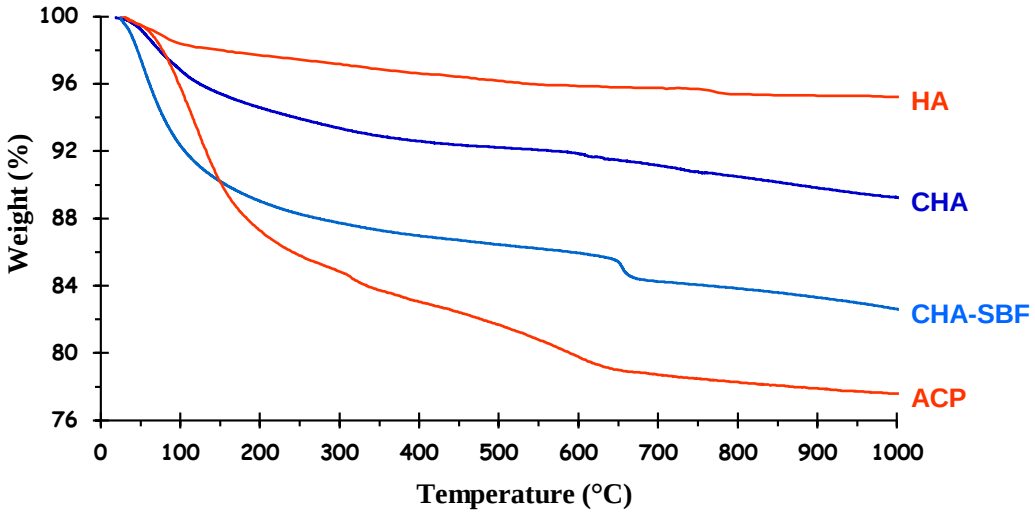

Figure S4. TGA weight-loss curves of the synthetic calcium phosphate samples: stoichiometric apatite (**HA**); biomimetic apatites (**CHA** and **CHA-SBF**); and amorphous calcium phosphate (**ACP**).

Figure S5

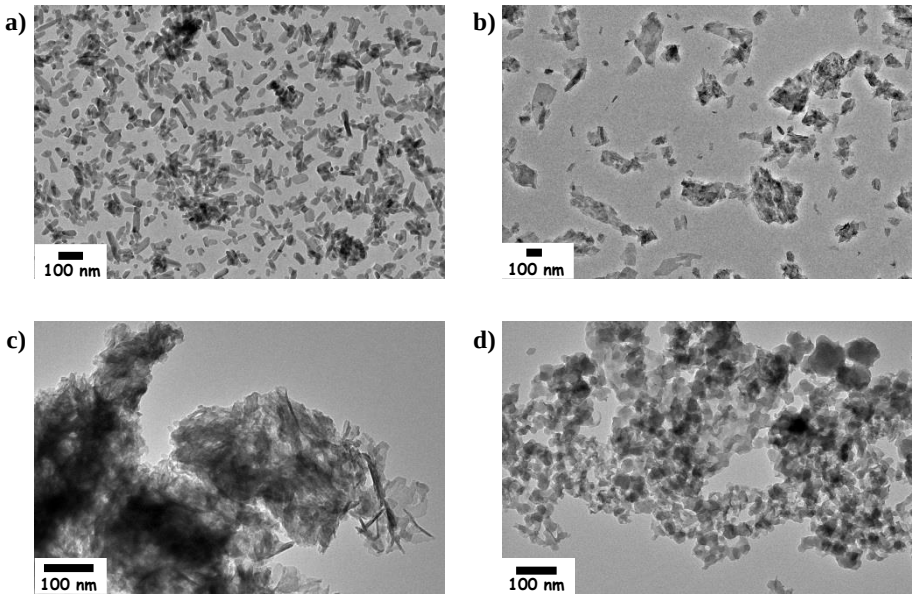

Figure S5. TEM images of the synthetic calcium phosphate samples: a) stoichiometric apatite (**HA**); biomimetic apatites, b) **CHA** and c) **CHA-SBF**; and d) amorphous calcium phosphate (**ACP**).

Figure S6

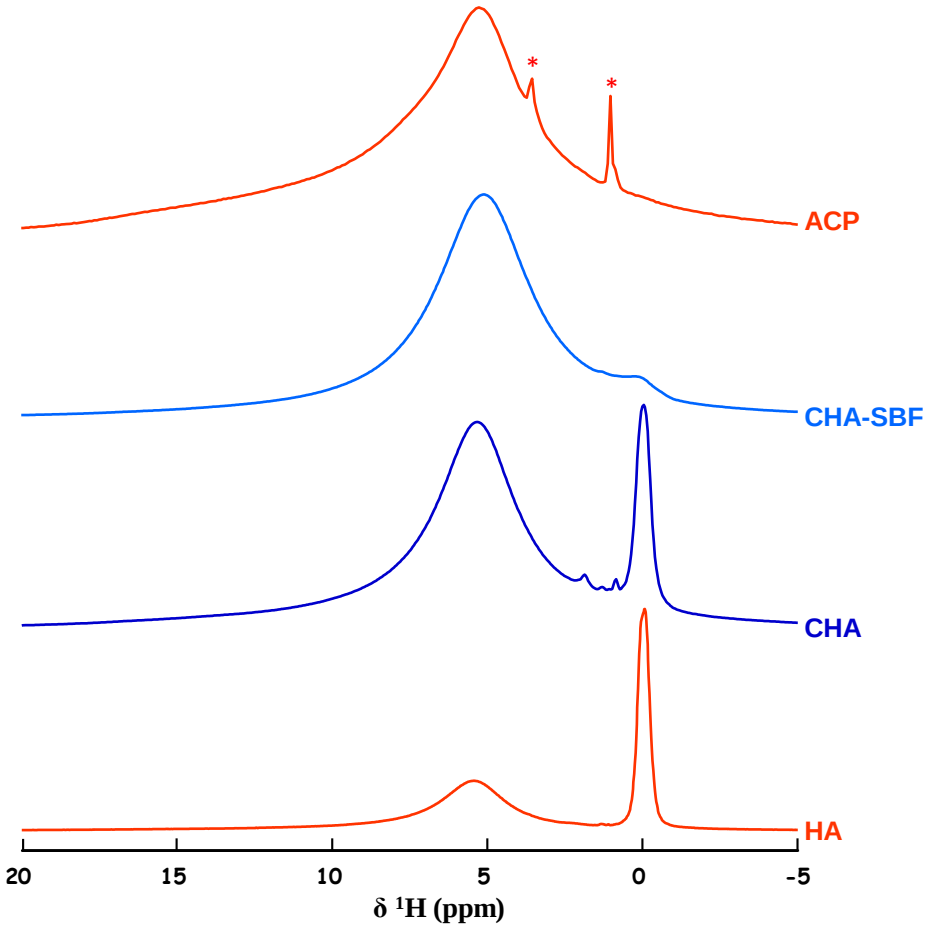

Figure S6. One-pulse ^{1}H MAS NMR spectra of the synthetic calcium phosphate samples: stoichiometric apatite (**HA**); biomimetic apatites (**CHA** and **CHA-SBF**); and amorphous calcium phosphate (**ACP**). The two narrow resonances in the ACP spectrum (see red asterisks) are due to the presence of ethanol.

Figure S7

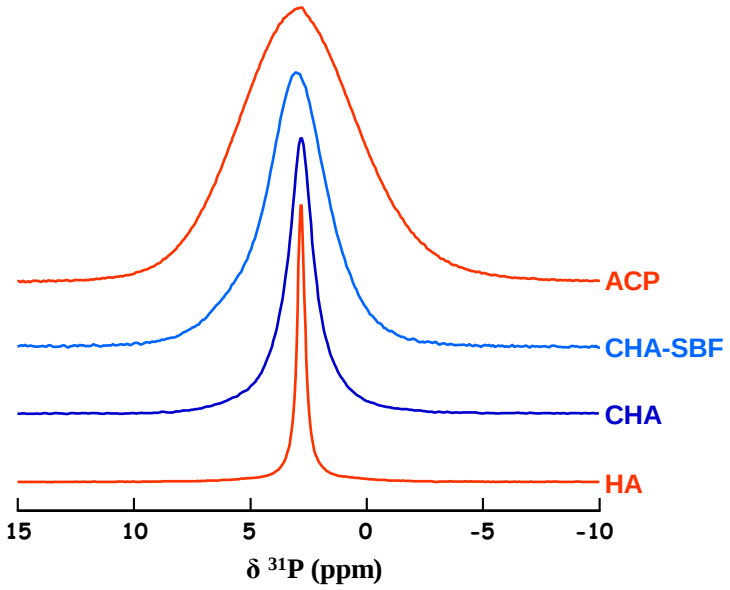

Figure S7. One-pulse ^{31}P MAS NMR spectra of the synthetic calcium phosphate samples: stoichiometric apatite (**HA**); biomimetic apatites (**CHA** and **CHA-SBF**); and amorphous calcium phosphate (**ACP**).

Figure S8

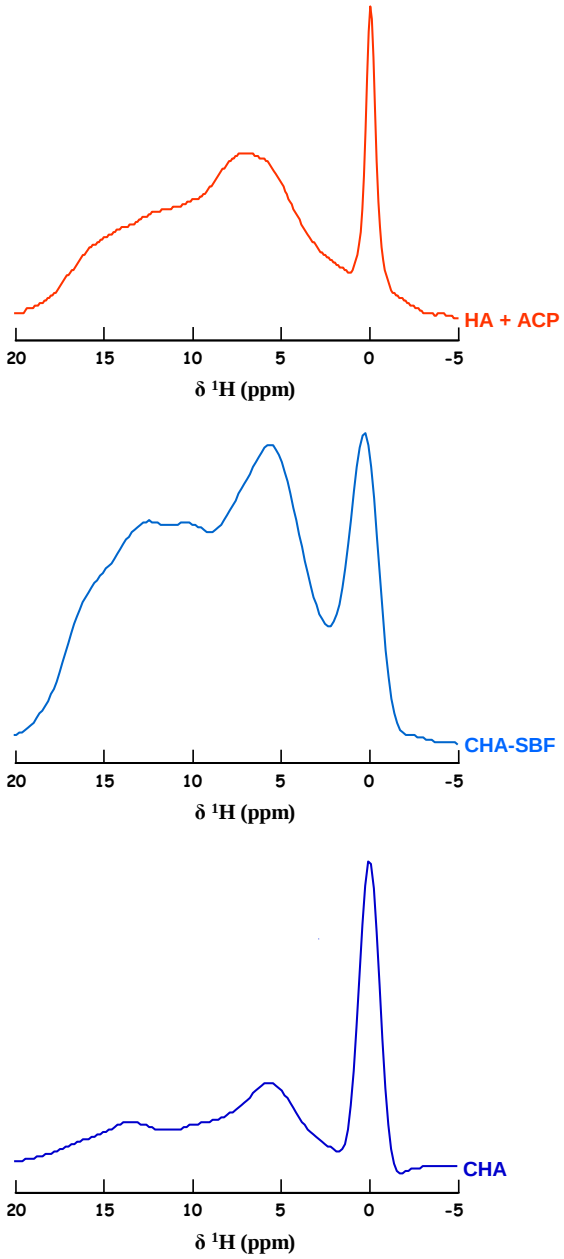

Figure S8. Double CP $^{1}H \rightarrow ^{31}P \rightarrow ^{1}H$ MAS NMR spectra of the physical mixture of HA and ACP powders (**HA/ACP mixture**), and the biomimetic apatites **CHA** and **CHA-SBF**. Contact times, $t_{CP}1$ = 1000 µs and $t_{CP}2$ = 850 µs.

Figure S9

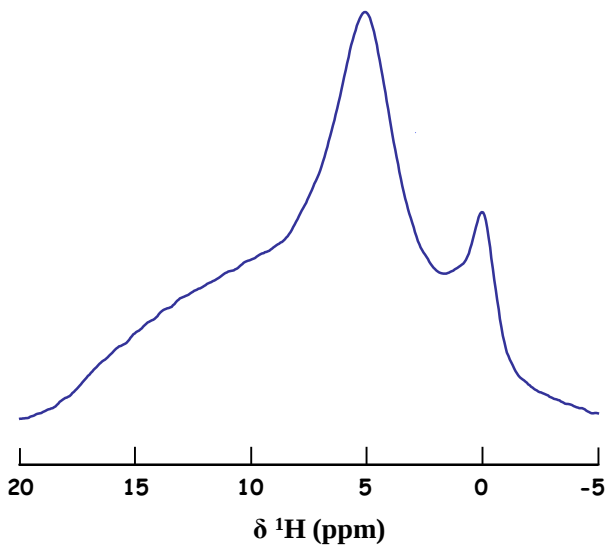

Figure S9. Double CP $^{1}H \rightarrow ^{31}P \rightarrow ^{1}H$ MAS NMR spectrum of a mature **bone** tissue sample originating from a two-years old sheep. Contact times, $t_{cp}1$ = 1000 µs and $t_{cp}2$ = 850 µs.

Figure S10

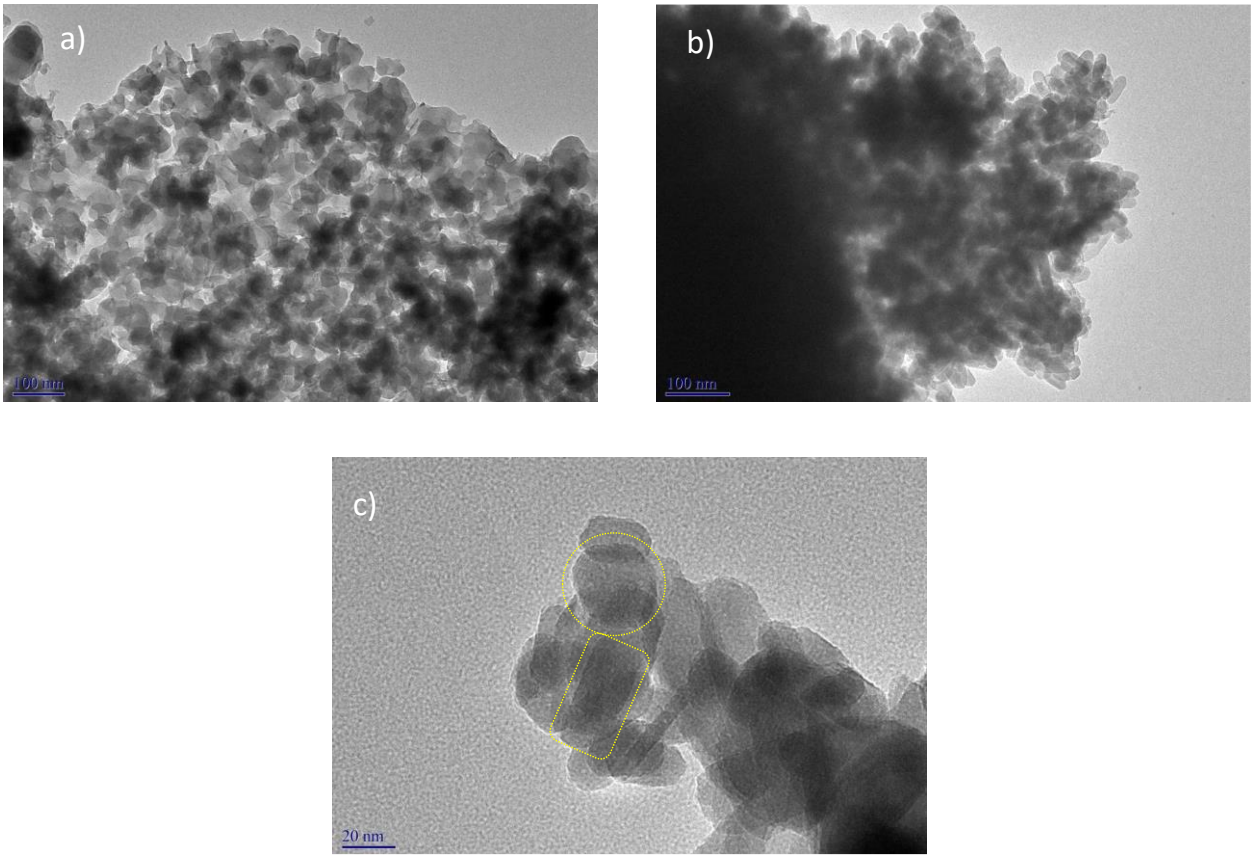

Figure S10. TEM images of the physical mixture **HA** + **ACP** displaying: a) microsized aggregates of **ACP**; b) microsized aggregates of **HA**; and c) locally **HA** (rode-like particle with visible crystallographic plans) and **ACP** (sphere-like particle) particles close to each other.

Figure S11

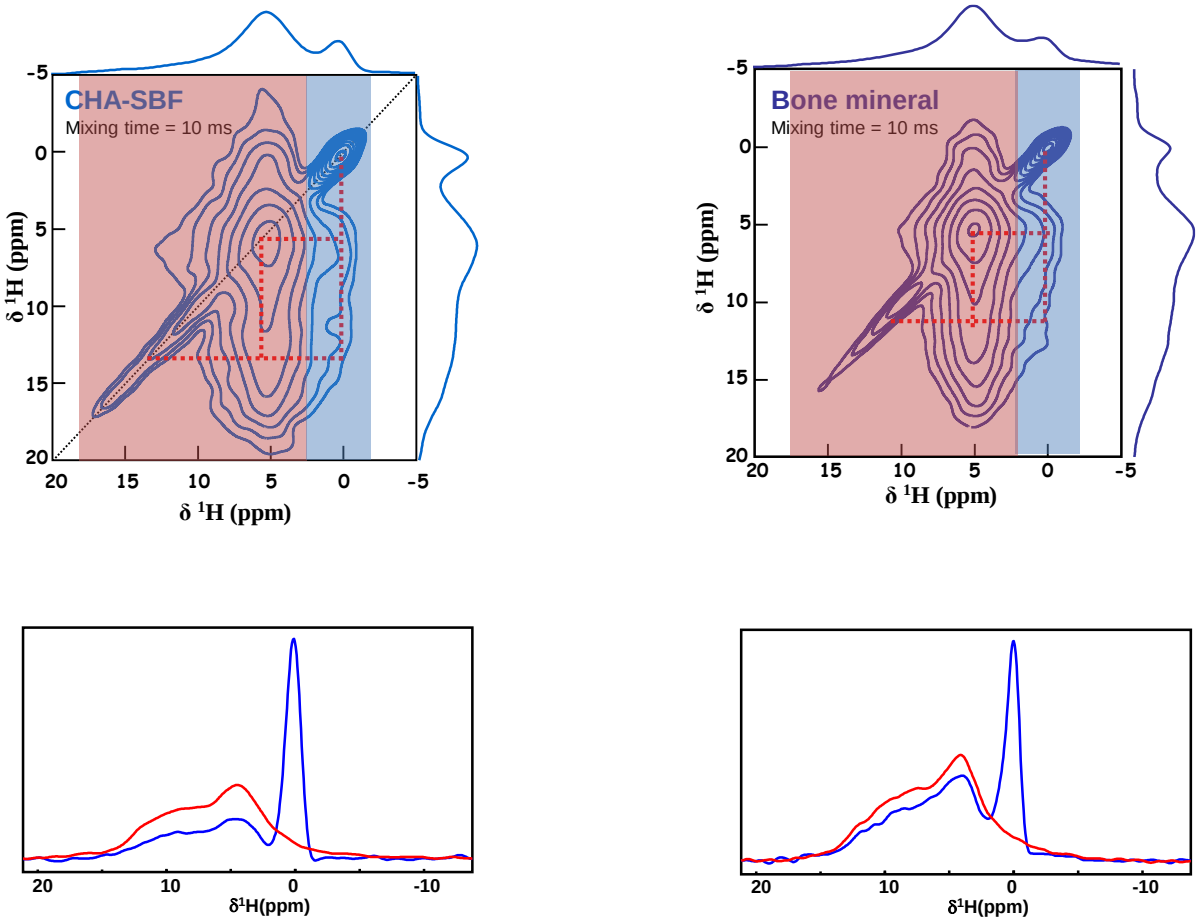

Figure S11. Comparison of the ^{1}H-^{1}H spin diffusion intensities in the ACP (sum of the ^{1}H signal in F1 dimension in the red region) and in the apatitic (sum of the ^{1}H signal in F1 dimension in the blue region) region from the 2D ^{1}H Double CP EXSY MAS NMR spectra of bone mineral and **CHA-SBF** (tmix = 10 ms). For the bone sample, we found that 45% of the total ^{1}H magnetization of the ACP-like domain was exchanged with the OH^{-} from the apatitic domain. For the biomimetic apatite **CHA-SBF**, the proportion is a little bit less as we found 36%.

Table S1. Position and linewidth of the ^{31}P NMR resonances for the various samples studied in the paper. N/A = not applicable.

	one-pulse ^{31}P NMR		**cross polarization ^{31}P NMR**			
			apatitic environments		non-apatitic environments	
Sample	$\delta(^{31}P)$ ± 0.1 ppm	LW ± 20 Hz	$\delta(^{31}P)$ ± 0.1 ppm	LW ± 20 Hz	$\delta(^{31}P)$ ± 0.1 ppm	LW ± 20 Hz
HA	2.8	80	2.8	80	N/A	N/A
CHA	2.9	200	3.0	140	3.1	430
CHA-SBF	3.2	370	3.1	290	3.2	660
Bone mineral	3.2	360	3.1	270	3.2	640
ACP	3.2	700	N/A	N/A	3.2	700